

Journal of Biomedical Optics

SPIEDigitalLibrary.org/jbo

Towards clinical use of a laser-induced microjet system aimed at reliable and safe drug delivery

Hun-jae Jang
Hyeonju Yu
Seonggeun Lee
Eugene Hur
Yoonkwan Kim
Seol-Hoon Lee
Naegyung Kang
Jack J. Yoh

Towards clinical use of a laser-induced microjet system aimed at reliable and safe drug delivery

Hun-jae Jang,^a Hyeonju Yu,^a Seonggeun Lee,^b Eugene Hur,^c Yoonkwan Kim,^c Seol-Hoon Lee,^c Naegyung Kang,^c and Jack J. Yoh^{a,*}

^aSeoul National University, Department of Mechanical and Aerospace Engineering, Seoul 151-742, Republic of Korea

^bB & B Systems, 481-10 Gasan-Dong, Geumcheon-Gu, Seoul 153-803, Republic of Korea

^cLG Household & Health Care R & D Center, 84 Jang-dong, Yuseong-gu, Daejeon 305-343, Republic of Korea

Abstract. An Er:YAG laser with 2940-nm wavelength and 250- μ s pulse duration is used to generate a microjet that is ejected at \sim 50 m/s in air. The strength of the microjet depends on the bubble dynamics from the beam–water interaction within the driving chamber as well as the discharging of the drug solution underneath the elastic membrane that separates the drug from the driving liquid. The jet characteristics, such as velocity, volume, and level of atomization, are obtained by high-speed camera images taken at 42,000 fps. The enhancements in jet volume (dosage) and repeated jet generation, which are aimed at making the injector suitable for general clinical applications, are achieved. The generation of repeated microjets is achieved with the help of a stepping motor that provides a uniform pressure within the drug reservoir before an ejection occurs through a micro nozzle. Also, two types of human growth hormones are used for monitoring any potential thermal damage to the drug solution due to a repeated laser ablation when driving the microjet. We provide strong evidence to support that the drugs, as they are injected to porcine skins, are free of the damage associated with the present delivery method. © The Authors. Published by SPIE under a Creative Commons Attribution 3.0 Unported License. Distribution or reproduction of this work in whole or in part requires full attribution of the original publication, including its DOI. [DOI: [10.1117/1.JBO.19.5.058001](https://doi.org/10.1117/1.JBO.19.5.058001)]

Keywords laser ablation; microjet; drug delivery.

Paper 140045R received Jan. 28, 2014; revised manuscript received Mar. 29, 2014; accepted for publication Apr. 29, 2014; published online May 21, 2014.

1 Introduction

There have been calls for a new drug delivery system to overcome common issues such as needle phobia and contamination from reuse of needles.^{1–3} One possible remedy is a system based on the microjet,^{4–9} whereby the generation of needle-free injection relies on the bubble dynamics within the injector.^{10,11} Both jet characteristics and bubble behavior determined by the laser beam properties such as wavelength and pulse duration have been studied.⁹ For general use of a laser-induced microjet injector as a clinical device, the delivery of drugs into the human tissue must be assured by a zero side effect associated with any type of drug damage done by strong thermal and inertial effects of the laser ablation-based mechanism for ejecting a microjet.⁸

In order to address these potential concerns addressed by the medical practitioners, the injector design is evolved around the use of two separate chambers that independently contain driving water (in the upper chamber) and the drug (in the lower reservoir), separated by a thermally resistant silicon rubber membrane. The laser ablation occurs within the upper driving chamber only, whereas the drug solution beneath the membrane is protected from the laser ablation. The strong bubble generation in the driving chamber gives rise to an elastic deformation of the membrane which then causes an instantaneous ejection of the drug solution from a drug reservoir through a narrow micro nozzle.

The maximum recommended therapeutic dose from the food and drug administration ranges from 0.00001 (epoprostenol) to

1000 (glycerol) mg/kg-bw/day.¹² These optimal amounts imply that the dose controllability is critical for a practical drug delivery system. Two ways to optimize dose controllability are a direct control of each ejected volume and a control of the number of repetitions with a fixed injection volume. Our system is geared toward the second way, in order to avoid pain or bruising due to an excessive amount of drug being transferred to the sensitive skin layer.^{3,13,14}

In this paper, we detail how the injection volume responds to the system parameters in order to achieve the practical dose (\sim 1 cc) of drug delivery possible for a general clinical use of the present system. Then a description of the repeated microjet generation using a step motor that provides a continuous refill of the targeted dose to the injector is provided. In addition, any potential thermal issues associated with the laser ablation-based drug delivery are analyzed via chemical analysis. Any damage done to the drugs is estimated by monitoring the increased rate in the amount of laminin and elastin of each corresponding epidermal growth factor (EGF) and human growth hormone (HGH) injected. The level of EGF and HGH is shown to remain unchanged before and after multiple injections, indicating that potential drug damage can be neglected in the present drug delivery system.

2 Materials and Methods

A microjet is generated by an expansion of the vapor bubbles induced by the focused laser beam as illustrated in Fig. 1(a).⁹ The jet characteristics are obtained from the high speed camera images taken at 42,001 fps [Fig. 1(b)]. An Er:YAG laser is used to generate vapor bubbles, and the wavelength and pulse

*Address all correspondence to: Jack J. Yoh, E-mail: jjyoh@snu.ac.kr

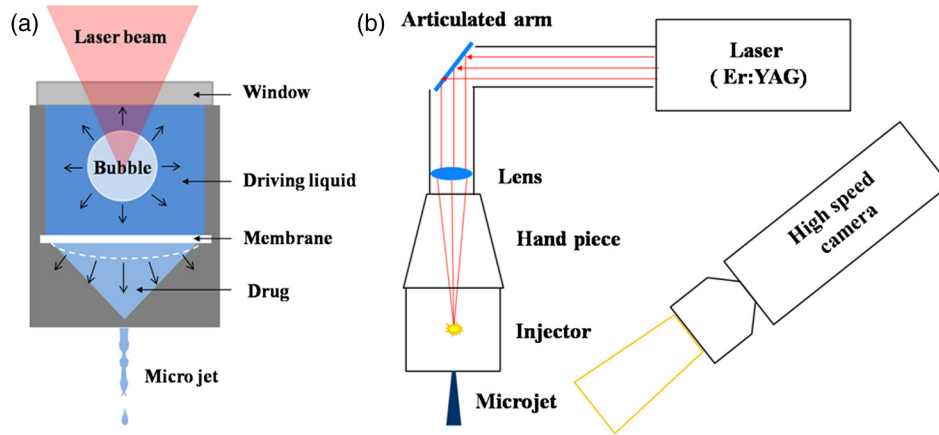


Fig. 1 (a) Mechanism of microjet generation and (b) a schematic of experiment.

duration of the beam are 2940 nm and 250 μs, respectively. The laser is operated at 10 Hz with 408 mJ energy in all tested cases.

The experimental objectives are twofold: one is an enhancement of the jet volume with a multiple jet generation capability, and the other is a safety assurance of the drug being injected by a laser ablation means. The parametric study is carried out to establish a relationship between the jet characteristics and the injector parameters. The injector is a pressurized device whose performance depends on its driving chamber height. The jet generation is directly related to the geometry of a drug reservoir as shown in Fig. 2(a). The jet volume and velocity are affected by reservoir diameter, reservoir angle, and cylinder height.

The experimental conditions are tabulated in Table 1. For repeated jet generation, a linear stepping motor (model name: 25BYZ-B04, Changzhou Fulling Motor Co., Jiangsu, China) is used to provide a continuous refill of the drug reservoir. Figure 2(b) is a schematic of the drug refill system that

consists of six components: control box, articulated laser arm, stepping motor, hand piece, syringe, and injector. Approximately 1 cc dose of the drug is contained in a syringe which is then fed to the drug reservoir. The laser beam is focused into a water chamber through a convex lens positioned inside the articulated arm, and the injector is connected through a hand piece. After the jet ejection, the step motor refills the drug by controlling the pulse signal as shown in Fig. 2(c).

Channel 1 shows the trigger signal of the laser, and channel 2 shows the control signal of the stepping motor as shown in Fig. 2(c). The motor moves 5.2 μm forward and the amount of the transferred drug is 0.46 μL on a single signal pulse of the stepping motor. The number of signal pulses can be adjusted by a controller to achieve a desired amount of the drug refill. These two signals are synchronized for a repeated refill process. A control box has the PCB panel which controls the signal of the stepping motor to a specified amount of drug being refilled.

EGF and HGH are the hormones used to assess any thermal damage done to the drug being injected. The molecular weights of EGF and HGH are 6 and 22 kD, respectively. Keratinocyte and fibroblast are cultured in plates, and these hormones are then diluted in each cell. After 24 h, RNA is extracted to investigate the gene expression for each cell (real time polymerase chain reaction). The level of gene expression for lamininin keratinocyte and that of elastin in fibroblast per concentration is analyzed, and the activity of the growth factor and hormone are checked before and after each injection.

3 Enhancement of Ejected Volume of Microjet

Ten experiments are conducted to investigate the effect of injector parameters on the jet characteristics. The experimental results are summarized in Table 2. Comparing cases 2, 6,

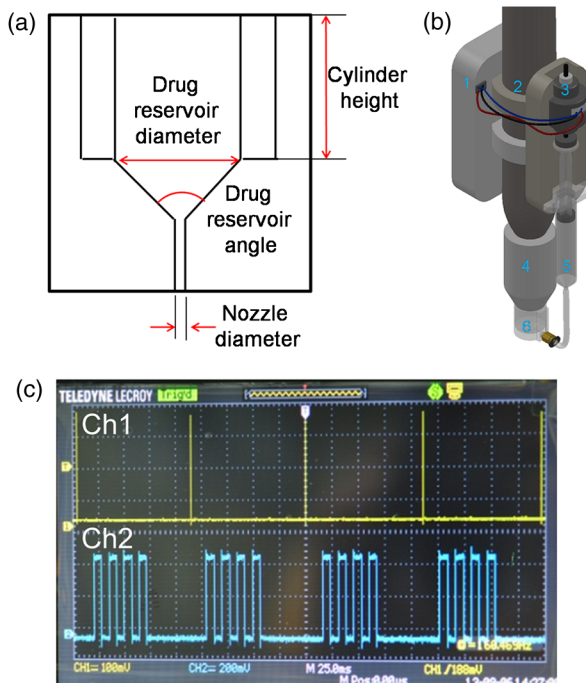


Fig. 2 (a) 2-D schematic of injector, (b) 3-D schematic of drug refill system, and (c) typical signals of laser and motor.

Table 1 Parameters of the microjet injector.

| Injector parameter | Value |
|-------------------------|--------------------------|
| Drug reservoir diameter | 4, 7, 11 mm |
| Drug reservoir angle | 30, 60, 90, 120, 150 deg |
| Cylinder height | 3, 5 mm |
| Confinement | Sapphire window |

Table 2 Experiment results for enhancement of the ejected jet volume.

| Case | Drug reservoir diameter | Drug reservoir angle (deg) | Drug reservoir volume (μL) | Cylinder height (mm) | Nozzle diameter (μm) | Jet velocity (m/s) | Jet volume (nL) |
|------|-------------------------|----------------------------|---|----------------------|-----------------------------------|--------------------|-----------------|
| 1 | 4 | 90 | 14.7 | 3 | 150 | 43.9 ± 1.7 | 640 ± 50 |
| 2 | 4 | 90 | 14.7 | 5 | 150 | 44.6 ± 1.8 | 468 ± 30 |
| 3 | 7 | 30 | 167.6 | 5 | 150 | 23.1 ± 1.0 | 452 ± 37 |
| 4 | 7 | 60 | 77.8 | 5 | 150 | 33.7 ± 2.6 | 832 ± 19 |
| 5 | 7 | 90 | 44.9 | 3 | 150 | 50.6 ± 1.6 | 2100 ± 28 |
| 6 | 7 | 90 | 44.9 | 5 | 150 | 50.2 ± 1.5 | 1738 ± 12 |
| 7 | 7 | 120 | 25.9 | 5 | 150 | 29.1 ± 3.0 | 584 ± 11 |
| 8 | 7 | 150 | 12 | 5 | 150 | 23.0 ± 4.0 | 358 ± 14 |
| 9 | 11 | 90 | 110.9 | 3 | 150 | 33.8 ± 1.9 | 1073 ± 16 |
| 10 | 11 | 90 | 110.9 | 5 | 150 | 29.5 ± 1.8 | 738 ± 12 |

and 10, an optimal diameter of the drug reservoir is determined to be 7 mm. The effect of the diameter is related to the bubble behavior. The microjet is generated by deformation of the membrane, which is strongly related to the size of the bubble. The area under pressure is determined by the cross sectional area of the bubble. If the cross section of a drug reservoir is smaller than the area under pressure, there must be a pressure loss and the ejected volume of the jet may become smaller. In the opposite case, if the pressure is not enough to expand the membrane, the volume of the jet being ejected may be decreased. These relations imply that an optimal value of a reservoir diameter exists, which is determined to be about 7 mm in the present experiment.

Comparing the cases from each group, one can understand the effect of the cylinder height on the resulting microjet: group 1 (case 1 and case 2), group 2 (case 5 and case 6), and group 3 (case 9 and case 10). In each group, an enhanced jet volume is achieved by the smaller cylinder height as shown in Fig. 3(a). The pressure inside the smaller driving chamber is higher than that of a larger volume when the microjet is ejected. The size of a generated bubble is the same for all cases because of the same laser energy (408 mJ) used, but a higher chamber pressure resulted in a smaller chamber volume.

The effect of the drug reservoir angle on the jet characteristics is shown with cases 3, 4, 5, 7, and 8. How the drug reservoir angle affects the jet can be found in Fig. 3(b), as an optimal value of the angle can be estimated to exist between 60 and 90 deg. The angle is proportional to a distance between a membrane and a nozzle with a fixed diameter of the drug reservoir. The membrane cannot stretch up to a maximum length when the distance is too short. Thus, a maximum volume of the ejected jet can be obtained at a specified distance according to an optimal angle.

4 Repeated Microjet Generation

Figure 4 corresponds to repeated microjet generation without a refill pump. Atomization starts from the third ejection while the jet volume is decreased as the number of injections increases. These phenomena are the result of air inflow through the nozzle. A microjet is generated by deformation of the membrane as the

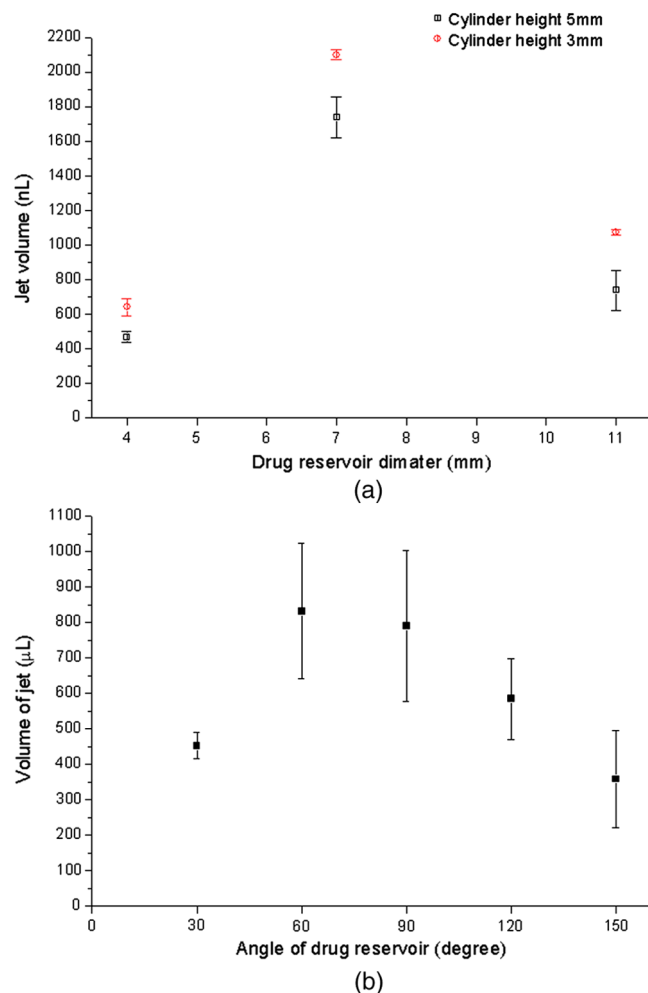


Fig. 3 Resultant jet volume due to (a) drug reservoir diameter and cylinder height and (b) angle of drug reservoir.

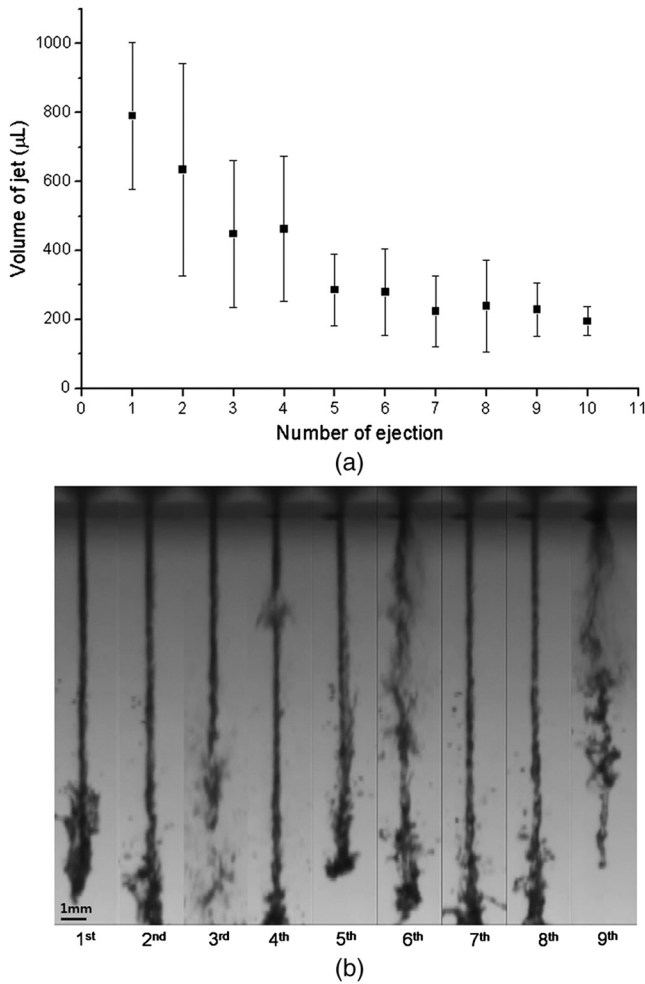


Fig. 4 Repeated microjet jets without the refill pump: (a) jet volume and (b) images of repeated microjet.

membrane regains its initial position due to its elastic property. During this process, pressure inside of a reservoir is lower, allowing air to enter from the outside. Consequently, a membrane squeezes out both the drug and air bubbles. When air bubbles form within a jet, rapid atomization occurs as the ejecting jet becomes very unstable.

For repeated jet generation, air inflow is minimized in order to reduce the level of atomization. One controls the flow rate of the drug using a motor-driven pump. A motor moves $41.7 \mu\text{m}$ in each step, and one step angle is controlled by eight clock signals. As a result, a motor moves $5.2 \mu\text{m}$ forward for each pulse signal. Figure 5 shows a trigger signal of the laser (ch 1) and a signal of the motor (ch 2). There exist two critical flow rates that define the three distinct regions of the jet. If the flow rate at which the drug chamber is being refilled by the motor is greater than the rate of ejection of the microjet, it defines the first critical flow rate. This is where the nozzle tip droplet gradually grows. If the flow rate is further increased, the droplet is detached with an increased ejection of the jet volume. This is denoted as the second critical flow rate.

Figure 5 shows the motor signal of each critical flow rate. Each number of pulse is 3 and 15, respectively, in one cycle. The laser is operated at 10 Hz, which means that signal has 10 cycles in 1 s. In the first critical flow rate, the motor moves $15.6 \mu\text{m}$ forward during 0.1 s, pushing in the syringe

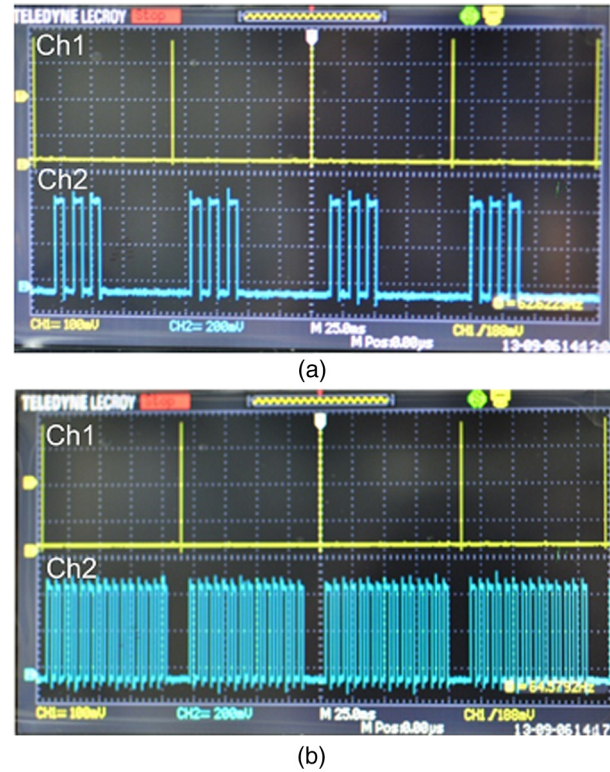


Fig. 5 Motor signals for (a) first critical flow rate ($13.8 \mu\text{L/s}$) and (b) second critical flow rate ($68.8 \mu\text{L/s}$).

plunger which is 10.6 mm in diameter. Thus, a total volume of a refilled liquid is $1.38 \mu\text{L}$ in each cycle. An averaged ejected jet volume is 832 nL and this value is smaller than the first critical flow rate. If the flow rate is increased, then the jet characteristics are changed by reaching a second critical flow rate. At this point, the motor moves $78 \mu\text{m}$ and the volume of the transferred liquid is $6.88 \mu\text{L/cycle}$.

The jet characteristics can be separated into three distinct cases. Case I is where the flow rate is less than the first critical flow rate. Case II is where the flow rate is between the first and the second critical flow rates. Case III is where the flow rate is greater than the second flow rate. In Case I, the flow rate is relatively low thus the air inflow is still allowed. Small sized droplets occur at the nozzle tip, which is shown by the line (denoted 1) in Fig. 6. In this case, the droplet size remains the same while the jet breaks up into smaller droplets. In Case II, the shape of a jet head is more stable than the first case as shown in Figs. 6(a) and 6(b), because the rate of air inflow is slowed down by the increment of the mass flow. But the bigger sized droplets are located at the nozzle tip and the size is increased by the greater flow rate. When the surface tension between the droplet and nozzle tip no longer sustain the weight of the droplet, the droplet is detached from the injector. The jet passes through the droplet, which makes the jet diameter thicker as shown in Fig. 6(b). For Case III, the droplet at the nozzle tip is minimized such that the inertia of an ejecting jet is greater than the surface tension between the nozzle tip and droplet. Therefore, the ejected jet is not easily disturbed by the presence of the droplet, which makes a narrower microjet.

Figure 7 shows three cases of the repeated microjets with respect to each flow rate. The jet volume in Case I is similar to that of Case III, while a relatively smaller volume of jet is

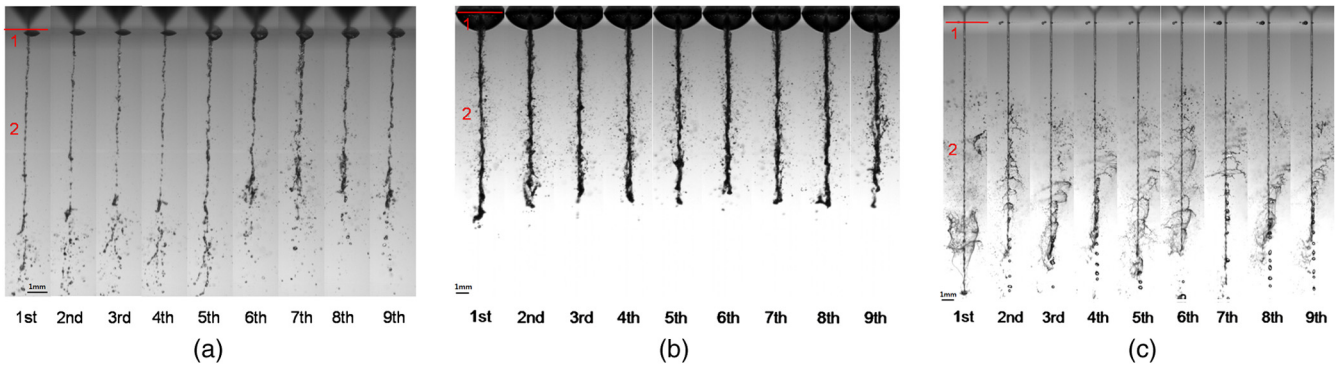


Fig. 6 Images of ejected jet according to the flow rates (a) Case I, (b) Case II, and (c) Case III.

observed in Case II because the droplet formed at the nozzle tip affects the jet characteristics in an adverse way as described earlier. The delivered amount of jet on an average is from 962 to 1415 nL/pulse. If the ejection is continuous for about 15 min and the laser is operated at 10 Hz, then the total ejection volume would reach 865.8 μ L to 1.273.5 mL. This means that the injector can deliver a targeted dose of \sim 1 cc which would fulfill most of the clinical requirements for various drugs.

The Droplet causes deceleration of a jet as follows: a viscous force causes jet deceleration if the jet is inside the droplet. Then the jet bursts out through the droplet, and the jet velocity is

decreased. These effects play a key role when the droplet reaches a certain size. The level of deceleration of a jet is determined by the size of a droplet. As a result, jet velocity is fastest in the order of Case III > Case I > Case II.

An Er:YAG laser whose wavelength is 2940 nm shows its highest absorption coefficient in the water. Thermal effects such as conduction or diffusion are dominant. This is a potential drawback of a drug delivery system if not properly treated.

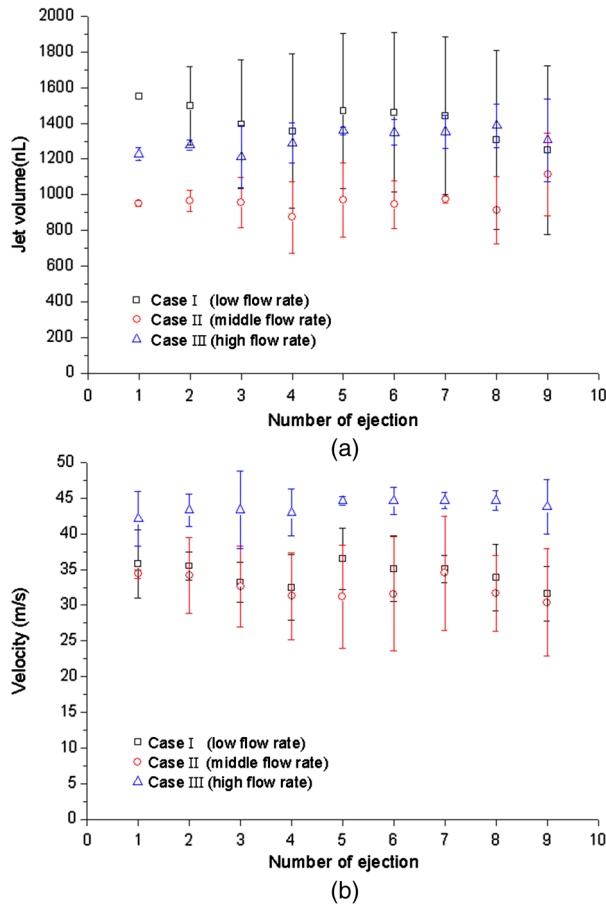


Fig. 7 Relationships between (a) ejected volume of jet and flow rate of drug refill and (b) between jet velocity and flow rate.

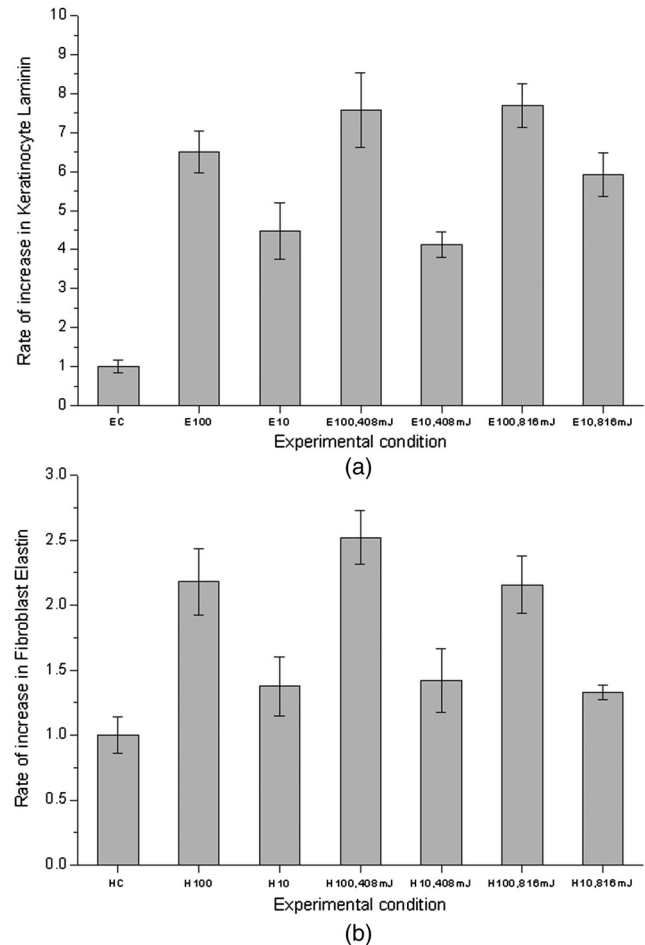


Fig. 8 Rate of increase in (a) epidermal growth factor and (b) human growth hormone. EC and HC are comparison groups. Numbers (100, 10) indicate the concentration in nanogram per milliliters. Laser energies (408 mJ, 816 mJ) are also shown.

Growth hormones, namely EGF and HGH, are used to investigate the potential thermal damage done to drugs due to the repeated laser ablation. Figure 8 shows the rate of increase in the gene expression. EC represents an amount of laminin in a cell which is not treated with EGF. The value of EC is set to one as a reference value. HC denotes an amount of elastin in cell which is not treated with HGH. Likewise, the value of HC is set to 1. E10 and E100 are the concentrations of laminin in a cell treated with EGF of 10 and 100 ng/mL, respectively. Similarly, elastin concentration in a cell treated with HGH is denoted as H10 or H100. Four cases (E100 408 mJ, E10 408 mJ, H100 408 mJ, and H10 408 mJ) are considered: growth factor or hormones are contained in a drug reservoir and discharged using a 408 mJ Er:YAG laser. The jet containing the growth factor is injected into the cell and the amounts of laminin and elastin are analyzed. Other cases considered (E100 816 mJ, E10 816 mJ, H100 816 mJ, and H10 816 mJ) are done in a similar manner except the laser energy is 816 mJ. The level of the increase in the rate for jet generation (E100 408 mJ, E10 408 mJ, E100 816 mJ, E10 816 mJ, H100 408 mJ, H10 408 mJ, H100 816 mJ, and H10 816 mJ) is marked the same as that of the regular syringe injection (E100, E10, H100, and H10), as shown in Fig. 8. Here, one confirms that there is no thermal damage associated with injection via the present laser-induced microjet injector.

5 Conclusions

In this study, jet characteristics and injector parameters are analyzed in order to establish the optimal conditions of a laser-based microjet system. The use of a stepping motor allowed continuous refilling of the drug reservoir and uniform ejections of the repeated microjets. Then the drug delivery is confirmed by making sure that there is no thermal damage done to the dosed drugs (two kinds of human growth hormones tested) during and after the microjet injection into a porcine skin. In conclusion, this work contributes to the controlling of jet characteristics and safety assurances of the delivered drug, and is particularly aimed at general clinical use of the system in the near future.

Acknowledgments

We thank the Korea Research Foundation DOYAK-2010 (NRF-2010-0029125), ILJIN Electric Co., and LG Household & Health Care for financial support through IAAT at Seoul National University.

References

1. M. A. F. Kendall, "Needle-free vaccine injection," *Handb. Exp. Pharmacol.* **197**, 193–219 (2010).
2. M. R. Prausnitz and R. Langer, "Transdermal drug delivery," *Nat. Biotechnol.* **26**, 1261–1268 (2008).
3. S. Mitragotri, "Current status and future prospects of needle-free liquid jet injectors," *Nat. Rev.* **5**(7), 543–548 (2006).
4. V. Menezes, S. Kumar, and K. Takayama, "Shock wave driven liquid microjets for drug delivery," *J. Appl. Phys.* **106**, 086102 (2009).
5. D. A. Fletcher and D. V. Palanker, "Pulsed liquid microjet for microsurgery," *Appl. Phys. Lett.* **78**, 1933–1935 (2001).
6. A. Taberner, N. C. Hogan, and I. W. Hunter, "Needle-free jet injection using real-time controlled linear Lorentz-force actuators," *Med. Eng. Phys.* **34**(9), 1228–1235 (2012).
7. T. Han and J. J. Yoh, "A laser based reusable microjet injector for transdermal drug delivery," *J. Appl. Phys.* **107**, 103110 (2010).
8. M. Park et al., "Er:YAG laser pulse for small-dose splashback-free microjet transdermal drug delivery," *Opt. Lett.* **37**(18), 3894–3896 (2012).
9. H. Jang et al., "Laser-induced microjet: wavelength and pulse duration effects on bubble and jet generation for drug injection," *J. Appl. Phys. B* **113**(3), 417–421 (2013).
10. A. Vogel and S. Busch, "Shock wave emission and cavitation bubble generation by picosecond and nanosecond optical breakdown in water," *J. Acoust. Soc. Am.* **100**, 148–165 (1996).
11. J. Noack et al., "Influence of pulse duration on mechanical effects after laser-induced breakdown in water," *J. Appl. Phys.* **83**, 7488–7495 (1998).
12. U.S. Food and Drug Administration homepage, Maximum Recommended Therapeutic Dose (MRTD) Database, <http://www.fda.gov> (26 February).
13. P. N. Hoffman et al., "Intradermal vaccine delivery: will new delivery systems transform vaccine administration?," *Vaccine* **19**, 3197–3208 (2008).
14. G. E. Theintz and P. C. Sizonenko, "Risks of jet injection of insulin in children," *Eur. J. Pediatr.* **150**, 554–556 (1991).

Biographies of the authors are not available.